Biochimica et Biophysica Acta, 1060 (1991) 37–44

ADONIS 000527289100218G

BBABIO 43473

Apparent destabilization of the S_1 state related to herbicide resistance in a cyanobacterium mutant

Diana Kirilovsky [1], Jean-Marc Ducruet [2] and Anne-Lise Etienne [3]

[1] *Section de Bioénergétique, Département de Biologie Cellulaire et Moléculaire, URA 1290, CNRS, CEN-Saclay,* [2] *INRA-SBE / DBCM, Saclay, Gif sur Yvette and* [3] *CNRS, UPR 407, Gif sur Yvette (France)*

(Received 5 March 1991)

Key words: Photosystem II; Herbicide resistant mutant; Oxygen-evolving system; (Cyanobacterium)

In this work we describe a new phenotype of herbicide-resistant mutants. We have selected and characterized several metribuzin resistant mutants from *Synechocystis* 6714. We found that an increase in metribuzin resistance involved a cross-resistance with other herbicides. Therefore, the mutants could be classified in three groups: (1) metribuzin resistant; (2) atrazine and metribuzin resistant; (3) DCMU, atrazine and metribuzin resistant. Mutants which did not present cross-resistance were up to 25-fold more resistant to metribuzin than the wild type. We have studied the electron transfer properties of Photosystem II in these mutants using several techniques (oxygen emission, fluorescence, and thermoluminescence measurements). They presented modifications in the electron transfer between Q_A and Q_B, as was generally observed in most herbicide-resistant mutants previously studied. However, unexpectedly, one of these mutants, M_{30}, presented a modified oscillatory pattern of oxygen emission. After dark adaptation the maximum of the oscillation was shifted by one flash. The matrix analysis indicated that the shifted maximum of the oxygen sequence corresponded to an increased S_0 concentration in the dark-adapted state. In whole cells S_0 and S_1 are in equilibrium. This equilibrium is shifted in favor of S_0 in the M_{30} mutant. The mutation renders the S-states more accessible to cell reductants.

Introduction

Photosystem II (PS II) has an enzymatic capacity of plastoquinone reductase and water oxidase. The reduction of the plastoquinone pool occurs through a two electron gate mechanism. Q_B binds to a pocket on the D_1 protein (Q_B site). In this site Q_B^- becomes tightly bound and it is released after a second reduction and protonation as a quinol. It is then rapidly replaced by a quinone of the pool [1]. In whole cells of *Chlorella*, and cyanobacteria, the plastoquinone pool is partially reduced and there can be as much as 50% centers with Q_B^- [2]. In dark adapted chloroplasts the plastoquinone pool is mainly oxidized and no Q_B^- is detected in the dark [2].

The oxidation of two water molecules to one oxygen molecule occurs after four successive photoreactions and charge storage in Photosystem II [3]. In consequence, the oxygen evolving complex can be in five different redox states S_0–S_4 (the S states) [3]. The oxygen is released during the S_3 to S_0 transition in which S_4 is a transient state. In the light, S_0 to S_3 are equally populated. In the dark S_2 and S_3 decay back to S_1 in minutes [4]. In chloroplasts, S_0 is converted to S_1 very slowly ($T_{1/2} \simeq 20$ min) by interaction with the tyrosine Y_D of D_2, which is fully oxidized after illumination [5–7]. When reduced, Y_D will be reoxidized by S_2 and S_3 within seconds ($t_{1/2} \simeq 2$ s) [6,8]. Therefore, in chloroplasts the S_0 concentration is 25% or lower, and that of S_1 is 75% or higher. In whole cells of chlorellae or *Chlamydomonas* the apparent S_0 dark concentration is somewhat larger [9]. This apparent S_0 concentration larger than 25% can be due to a true equilibrium between S_0 and S_1 shifted towards S_0 in whole cells. It can also be due to the competition between the oxygen evolving complex and an electron donor on the first flash of a sequence.

Abbreviations: Chl, chlorophyll; DCMU, 3(3,4-dichlorophenyl)-1,1-dimethylurea; PS II, Photosystem II; Q_A and Q_B, primary and secondary quinone electron acceptors.

Correspondence: A.-L. Etienne, CNRS, UPR 407, Bât. 24, 91198 Gif sur Yvette, Cedex France.

The electron transfer between the primary (Q_A) and the secondary (Q_B) electron acceptors of PS II can be blocked by several herbicides [10]. They bind in the same region of the D_1 protein as Q_B [11]. All the mutants reported until now, presented a drastic decrease of the herbicide affinity for its binding site, produced by different mutations of the D_1 protein. These mutations are also related to an increase of the Q_A^- concentration in the steady state due to a decreased equilibrium constant for the reaction $Q_A^- Q_B \leftrightarrow Q_A Q_B^-$ [13–16]. Some herbicide resistant mutants present a slower reoxidation of Q_A^- by Q_B [17].

Our group has already described the phenotypes of different herbicide resistant mutants of *Synechocystis* 6714 (a cyanobacterium) selected in the presence of DCMU, atrazine or ioxynil [15,18–21]. Their phenotypes were compared to that of other species (higher plants or *Chlamydomonas reinhardtii*) [21]. Three types of mutation affecting electron transport of PS II were described: (1) mutations which produce small effects on electron transport and weak herbicide resistance [17,19,20], (2) mutations leading to a high herbicide resistance and to an increased steady-state concentration of Q_A^- which is not linked to a slower initial rate of Q_A^- reoxidation [18,22]; (3) mutations which decrease the reoxidation rate of Q_A^- by Q_B with no appreciable effect on the steady-state concentration of Q_A^- [17,24].

In this work we describe a new phenotype of herbicide resistant mutants. A mutant of *Synechocystis* 6714 selected in the presence of metribuzin presented modifications in the dark S states distribution of PS II in addition to small modifications of the electron transfer between Q_A and Q_B.

Materials and Methods

Growth conditions

Synechocystis 6714 cells were grown in the mineral medium described by Herdman et al. [24] with twice the concentration of nitrate and an illumination of about 70 $\mu E/m^2$ per s. The cells were grown at 34°C. Other conditions were as previously described [15].

Mutant selection

Synechocystis 6714 cells in the log phase of the growth (about 10^8 cells/ml) were spread on agar plates containing different concentrations of metribuzin: 10^{-3} M, $5 \cdot 10^{-4}$ M, $2 \cdot 10^{-4}$ M, 10^{-4} M, $5 \cdot 10^{-5}$ M and 10^{-5} M. The mutation frequency varied between 10^{-10} to $2 \cdot 10^{-8}$ from $5 \cdot 10^{-4}$ M to $5 \cdot 10^{-5}$ M metribuzin. After 3 weeks of light incubation at 34°C isolated colonies were picked out and subcloned. The purified mutants were grown in liquid medium in order to characterize their phenotypes.

Thylakoid preparation

Thylakoid membranes were isolated by a modification of the method described by Burnap et al. [25]. Cells were suspended in 50 mM Hepes-NaOH (pH 6.8), 5 mM $MgCl_2$, 5 mM $CaCl_2$ and 25% glycerol (v/v) solution (buffer A) (100–200 μg Chl/ml). After 1–2 h on ice cells were pelleted by centrifugation and resuspended in buffer A (100–200 μg Chl/ml) containing 50 μg/ml DNase and 1 mM each of caproic acid, benzamidine and PMSF. The cells were then broken in a Bead Beater (Biospec Products, U.S.A.) using 0.1–0.25 mm glass beads, for seven pulses of 20 s each, with 1 min cooling intervals. Glass beads and unbroken cells were separated from membrane suspension by pelleting at $1250 \times g$ for 5 min. The membrane fragments were pelleted by centrifugation at $28\,300 \times g$ for 1 h. The pellets were resuspended in a minimal volume of buffer A and stored at −80°C.

Fluorescence measurements

The fluorescence decay after a one-turnover saturating flash was measured in an apparatus already described [26]. A pulsed light emitting diode (645 nm) was used as a non-actinic detecting beam (the pulses were 2 μs, spaced at 16 μs). The set of filters was a 4-96 Corning filter in front of the short saturating flash and a combination of a KV 550 (Schott), a RG 5 and an interference filter centered at 685 nm in front of the photomultiplier tube (S 20 light sensitivity).

The material (1.5 μg Chl/ml) was dark adapted for at least 10 min and the sample was renewed before each recording. To get a good signal-to-noise ratio, the curve was averaged 20 times.

Oxygen measurements

The amount of oxygen produced per flash during a sequence of saturating flashes was measured with a rate electrode equivalent to that described by Joliot and Joliot [27]. The short (5 μs) saturating flashes were produced by a Strobotac (General Radio Company). The spacing between flashes was 0.6 s. Each experiment was started with dark-adapted cells (500 μg Chl/ml). The flowing medium was 50 mM Hepes-NaOH (pH 6.8), 5 mM $CaCl_2$, 0.1 M KCl as an electrolyte. The cells for the benzoquinone treatment, at a concentration of around 10 μg Chl/ml in their culture medium were incubated for some minutes in the presence of 10^{-3} M benzoquinone, they were then centrifuged and washed twice in the medium used during the oxygen measurements.

Thermoluminescence

The thermoluminescence cuvette, 1 mm thick, was formed by a rubber plate with a 1×2 cm cavity, pressed between a plexiglass window and an aluminium plate which could be dipped partly or totally in liquid nitrogen. A 'Thermocoax' heater, on the other side of the plate, was used for regulation of temperature which was measured in the cuvette by a thermocouple. For B band measurements the samples were

incubated 5 min in the dark, then a flash was given at −5 °C and the sample was rapidly cooled. For the detection of the Q band, DCMU was added after dark adaptation then a flash was given at −20°C.

After 30 s of temperature equilibration at −40°C, the temperature was linearly increased to +80°C in 4 min (0.5 C°/s). The luminescence emission was measured, at wavelengths above 650 nm, by a cooled photomultiplier connected to a photon counting system. Signal recording and temperature regulation were performed by a PC compatible microcomputer through plugged-in Analog/Digital and IEEE interface cards. The signal was treated by a computer program specially designed for analysis of thermoluminescence data.

Two noise-filtered curves were derived from the signal, one by Fourier transform, followed by inverse transform with low frequency components, another one by linear adjustment, which also provided the first derivative of the signal. These two curves were generally overlapping.

Estimation of the activation energy can theoretically be obtained from an Arrhenius plot of the rising edge of the TL band but the presence of minor TL bands in this region generally leads to erroneous evaluation of the activation energy. Therefore, a simulation procedure was developed, to adjust the number of traps n, the preexponential factor s and the activation energy E_A, using the Eyring equation, which was introduced by Vass et al. [28] in the analysis of TL emission:

$$L(T) = n \cdot s \cdot T \cdot e^{-E_A/kT} \quad (1)$$

where T is absolute temperature and k the Boltzman constant.

This equation was computed step by step, from low to high temperatures. Starting with n_0, which represents the area under the analyzed TL band, n was decreased, at each step, by the value of $L(T)$.

The computer-simulated curve was first graphically adjusted to the main TL band, using either the direct signal or the Fourier-filtered curves, in the temperature domain in which the first derivative did not point out the presence of minor bands (25–45°C). Then, a minimization procedure further adjusted the three parameters n_0, s, E_A to the selected part of the experimental signal.

In photosynthetic systems, the Eyring activation energy (E_A) for thermoluminescence emission is an apparent activation energy, since it depends not only on the recombination step which creates luminescence excitons, but also on the charge distribution on the electron carriers of the photosynthetic chain [29]. Although this simulation does not reflect a particular recombination step, it provides a characterization procedure for a TL band, more reliable than only taking into account the maximum of the peak.

EPR spectra

EPR spectra were recorded at liquid helium temperature with a Bruker ESR 200D X-band EPR spectrometer equipped with an Oxford Instruments cryostat as described by Boussac and Rutherford [30].

Results

Mutant selection and herbicide resistance

Spontaneous metribuzin resistant mutants were selected from wild-type *Synechocystis* 6714. Several herbicide concentrations varying between 10^{-3} M to 10^{-5} M were used in order to obtain different herbicide resistant phenotypes. The selected mutants could be classified in three groups. Table I shows the I_{50} average concentrations of different herbicides of the three groups of metribuzin resistant mutants. We found a correlation between mutant phenotypes and metribuzin concentrations used for their selection. Mutants resistant only to metribuzin were mostly obtained in the presence of 10^{-5} M–$5 \cdot 10^{-5}$ M metribuzin. The mutants selected with $5 \cdot 10^{-4}$ M were all DCMU, atrazine and metribuzin resistant. Mutants resistant to metribuzin and atrazine appeared with intermediary metribuzin concentrations. Therefore, an increase in metribuzin resistance involved a cross resistance with other herbicides.

One of the selected mutants, M_{30}, which was 20-fold resistant to metribuzin and did not present any cross resistance was further characterized.

Oxygen emission

In most oxygen evolving systems, after dark adaptation, the oscillations of oxygen produced per flash display a maximum amount on the third flash. This is classicaly attributed to a larger concentration of S_1 as compared to the concentration of S_0 in the dark adapted state.

Fig. 1 shows the oscillatory pattern of the mutant, M_{30}, and of wild-type cells. The two sequences were normalized to Y_m (mean value of Y) which is almost

TABLE I

Average I_{50} concentrations of different herbicides of three groups of metribuzin resistant mutants (a)

	I_{50} (M)			
	metribuzin	atrazine	DCMU	ioxynil
Wild-type	$2 \cdot 10^{-6}$	$3 \cdot 10^{-6}$	$5 \cdot 10^{-7}$	$2 \cdot 10^{-6}$
Type I	$\leq 5 \cdot 10^{-5}$	s	s	s
Type II	10^{-4}	$3 \cdot 10^{-5}$	s	s
Type III	$> 10^{-3}$	$5 \cdot 10^{-5}$	$3 \cdot 10^{-5}$	s

s, sensitive.

I_{50}, concentration of the herbicide needed to block half of the maximal variable fluorescence.

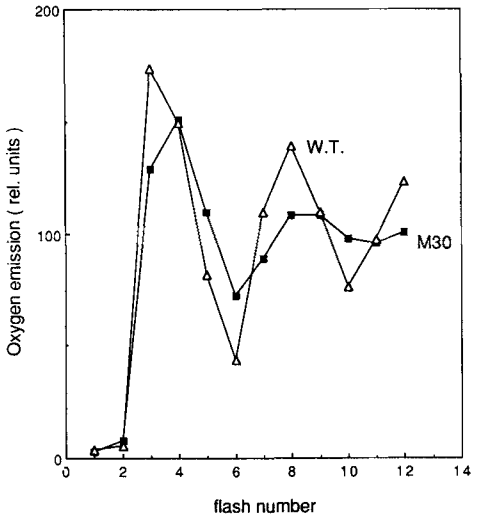

Fig. 1. Oxygen yield per flash during a series of short saturating flashes spaced at 0.6 s in wild-type (△——△) and M_{30} (■——■) cells. The sequences were normalized to Y_m (mean value of Y). The two sequences shown are individual sequences of each type representative of the two types of behavior. The computed values for these sequences are $\alpha = 0.17$, $S_0 = 49$ for the M_{30}, $\alpha = 0.14$, $S_0 = 35$ for the wild-type.

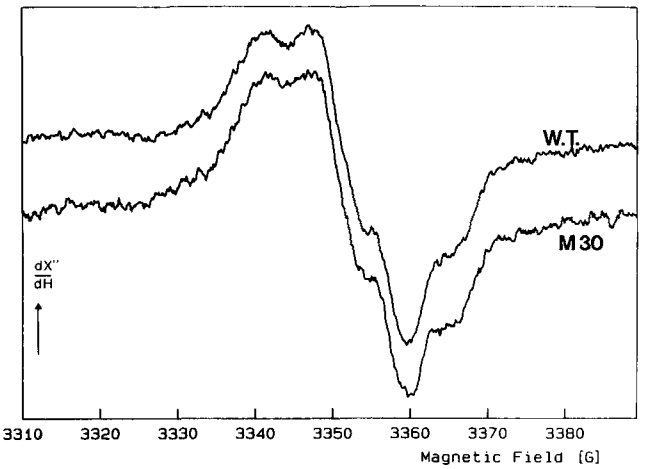

Fig. 2. EPR spectra of SII_s in wild-type and M_{30} cells after 5 min of dark adaptation. The chlorophyll concentration was 1.5 mg/ml. Instrument setting: temperature 20 K, modulation amplitude 2 G, microwave power 2 μW and signal gain $1.6 \cdot 10^6$. 16 accumulations of the signal were done.

stable along the sequence. The striking features of the oscillatory pattern of M_{30} were the low Y_3, which was smaller than Y_4 and the relatively small amplitudes of the oscillations around the Y_m value.

From the amount of oxygen produced per flash (Y_n) during a flash sequence, the 'sigma method' developed by Lavorel [9] is able to compute the miss and the double hit parameters, the initial S_0 and S_1 apparent values and the mean value for Y (Y_m). The different parameters for wild-type and M_{30} cells are shown in Table II. In the M_{30} mutant the miss parameter was slightly increased. The apparent concentration of S_0 in the dark was also increased in the mutant: the S-state distribution was about 50–60% S_0 and 40–50% S_1 in M_{30}, compared to 30–40% S_0, 60–70% S_1 in the wild-type.

TABLE II

The values of parameters computed by the matrix analysis [9] from the recorded oxygen sequences

The computations are done on the first nine flashes of a series. This gives for each sequence three values for σ_1, σ_2, σ_3 and Y_M. For simplicity the miss parameter (α) is considered to be the same for the different S state transition. The values vary in the limits given. This is due to various physiological parameters of the cells which vary with the different batches and during an experiment. Several sequences are done on the same sample which remains on the electrode for a rather long time (30 min to 3 h). The fit with a simulated sequence computed from the parameters obtained is good for the wild type, rather poor for the M_{30} mutant

	S_0	S_1	α	Y_M / Y_3
Wild-type	30–40	70–60	0.125–0.150	0.55–0.60
M_{30}	50–60	50–40	0.14 –0.20	0.8 –0.9

If the large concentration of S_0 was due to a diversion of positive charges from S_2 and S_3 to oxidize Y_D, then the EPR signal II slow (corresponding to Y_D^+) of the mutant should be lower than that of the wild-type and the shape of the flash sequence should depend on the flash frequency.

The amplitude of the signal II slow was the same in the M_{30} and wild-type cells (Fig. 2). The shape of the sequence was not dependent on the flash frequency (0.3 to 1 Hz) (data not shown). This shows that there is not a very fast reduction of S_2, S_3 occurring in the M_{30} mutant. Therefore, the phenomenon occurring in the M_{30} mutant was not due to the same mechanism as that occurring in the chloroplasts after a long dark period [6–8].

The apparent larger S_0 concentration in the mutant can either be due to a true shift towards S_0 for the $S_0 \leftrightarrow S_1$ dark equilibrium or to the oxidation of an electron donor not involved in the oxygen evolving complex.

We can study the rate of the apparent dark reduction of S_1 to S_0: one preflash will minimize the S_0 concentration and place the centers in the S_1 and S_2 states. Then during a following dark period S_0 will rapidly decay back to S_1 and eventually S_1 will decay back to S_0. We follow the variation of the Y_4/Y_3 ratio (indicative of the S_0/S_1 concentration) versus the dark time between the preflash and the flash sequence (Fig. 3). In the wild type the Y_4/Y_3 ratio reached a value close to 0.7 as soon as the deactivation of S_2 was achieved ($\simeq$ 50 s) and increased only slightly from 50 to 200 s dark time. In the mutant cells, 50 s after the preflash the Y_4/Y_3 was already higher than in the wild

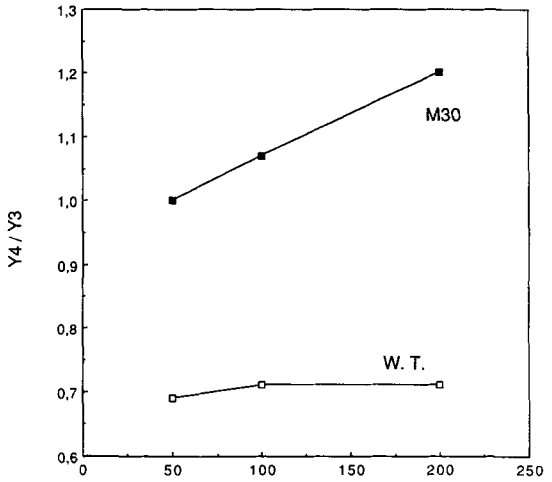

Fig. 3. Variation of the Y_4 / Y_3 ratio versus the dark time between a preflash and the flash sequence in wild-type (□ ——— □) and M_{30} (■ ——— ■) cells.

type and it increased steadily when the dark period was lengthened (Fig. 3).

If the apparent reduction of S_1 in the dark was due to the oxidation on the first flash of an accessory donor localized in the PS II reaction center, the same inversion of the Y_4/Y_3 ratio should be observed for the thylakoids isolated from the M_{30} cells. This was not the case, the thylakoid flash sequence exhibited a maximum on the third flash (not shown).

If S_1 was slowly reduced by a reductant present in the cell, a pre-treatment with benzoquinone might oxidize the reductant and change the S_0/S_1 ratio. This was indeed the case as shown in Fig. 4. There was also

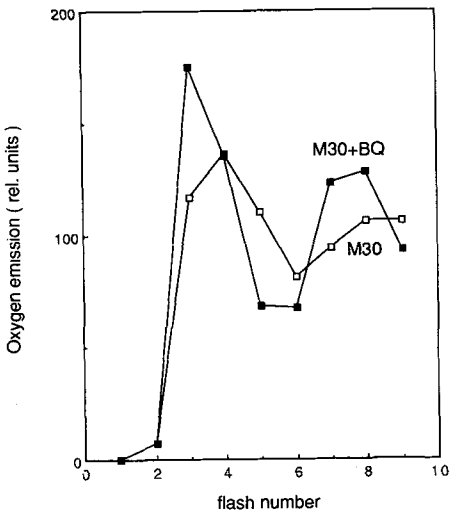

Fig. 4. Effect of a pretreatment with 10^{-3} M benzoquinone on the oscillation pattern of M_{30}. The cells were washed twice after the benzoquinone treatment and also for the control. Oxygen yield per flash in M_{30} cells after benzoquinone treatment (■ ——— ■); or without treatment (□ ——— □). The parameters computed from the sequences shown are: $\alpha = 0.141$, $S_0 = 53$ for the M_{30}, $\alpha = 0.135$, $S_0 = 36$ for the M_{30} after the benzoquinone pretreatment.

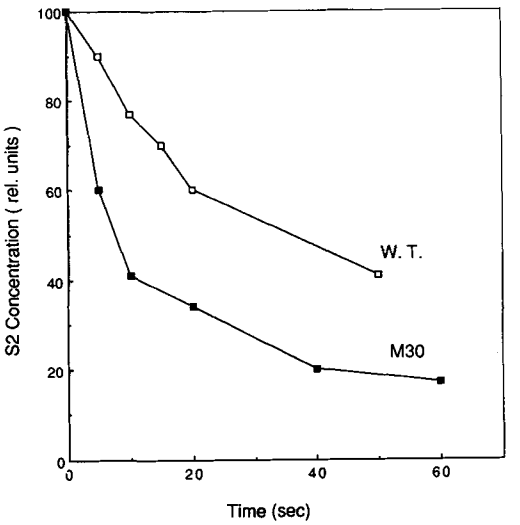

Fig. 5. Decay kinetics of the S_0 state in wild-type (□ ——— □) and M_{30} cells (■ ——— ■). The amount of S_0 was calculated from oxygen-yield sequences measured at 28°C after one preflash followed by various intervals of dark relaxation.

a decrease in the miss parameter of the M_{30} cells pre-treated with benzoquinone.

Electron transport between Q_A and Q_B

The M_{30} mutant presented a modification of the electron transfer from Q_A^- to Q_B in addition to the particular S_1, S_0 distribution in the dark. In all previously studied herbicide resistant mutants of *Synechocystis* 6714 the modification on electron transfer from Q_A to Q_B were negligible or resulted in a change in the apparent equilibrium constant (Q_A^-/Q_B^-) [21]. This change was correlated to a shift in the thermoluminescence B band, an accelerated S_2 deactivation, an increase in the miss parameter and a larger slow phase in the fluorescence decay after a flash [21].

S_2 deactivation and thermoluminescence

An electron which is stored in the acceptor side is shared between Q_A and Q_B in the equilibrium state. There will be an increase in the rate of the back reaction ($S_2Q_B^-$) if the probability for the electron to be on Q_A is increased. This rate was studied by S_2 deactivation followed by oxygen emission. The overall half-time of S_2 deactivation was about 20 s for the wild-type and about 8–10 s for the M_{30} (Fig. 5).

Samples which are progressively heated after a flash given at a low temperature have a luminescence emission in the temperature range allowing charge recombination [31]. The B band, which can be attributed to the $S_2Q_B^-$ (or $S_3Q_B^-$) recombination and the Q band, which is related to $S_2Q_A^-$ back-reaction [31,32] were compared in the wild-type and M_{30} mutant (Fig. 6). A large shift of the B band towards the low temperature was observed in the mutant as compared to the wild-

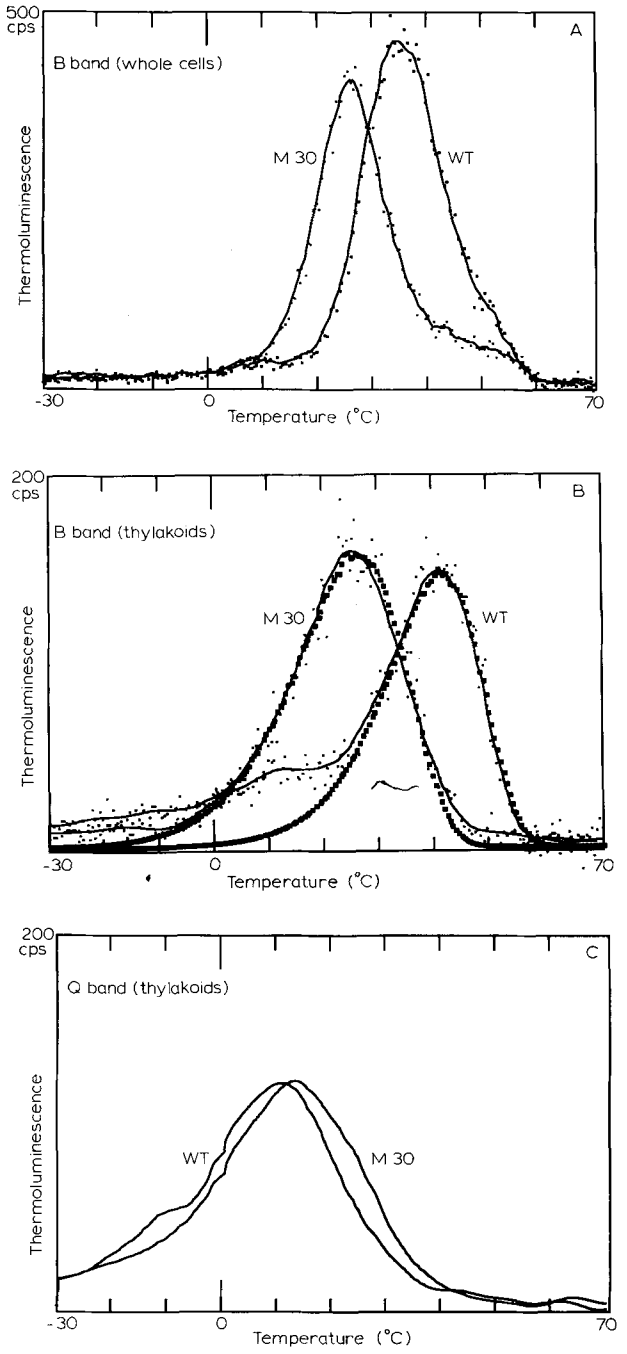

Fig. 6. Thermoluminescence emission of wild-type and M_{30}. B band in whole cells (A) and in thylakoids (B) after one turnover flash at $-5\,^{\circ}C$. Q band in thylakoids (C) after one turnover flash at $-20\,^{\circ}C$ in the presence of DCMU. ····· thermoluminescence signal; ——— Fourier filtered TL signal. ■ ■ ■ ■ in B, the simulation of the B bands with EA = 0.93 eV for the wild-type and EA = 0.73 eV for the M_{30} are also shown.

type in the cells and in the thylakoids (40°C to 25 °C). (Fig. 6A and B). The simulation analysis of the B band showed that the apparent activation energy of the $S_2Q_B^-$ recombination was lower (0.73 eV) in the M_{30} mutant than in the wild-type (0.93 eV) (Fig. 6B). The faster S_2 deactivation and the shift of the B band suggested that the back reaction $S_2Q_B^-$ was facilitated in the M_{30} mutant as compared to the wild-type. The presence of an inhibitor at saturating concentrations in the Q_B site suppress any effect of a mutation modifying only the Q_B niche. Under this condition we observed a small shift of the Q band towards higher temperatures (10°C to 13 °C) (Fig. 6C). This implies that the effect of the mutations of M_{30} is not restricted to the Q_B niche. It might also affect either Q_A/Q_A^- equilibrium or the donor side.

Since the only substrates for the B band are S_2 and S_3 recombining with Q_B^-, the amplitude of the B band oscillates with the S-states distribution. The oscillatory pattern of the B band is influenced by three factors: (a) $S_3Q_B^-$ recombination is twice as luminescent as $S_2Q_B^-$ [33,34]; (b) the miss parameter favor the damping of oscillations by mixing the S-states; (c) in whole cells of cyanobacteria the ratio Q_B/Q_B^- is close to 1 after dark adaptation [35]. The observation of a maximum after two flashes (Fig. 7) in the wild type is explained by the factors (a) and (c). The emission after two flashes results mostly from $S_3Q_B^-$ recombination since the concentration of S_1 is about 3-fold that of S_0 after dark adaptation. The B band oscillation was very small in the M_{30} mutant (Fig. 7). This result is in accordance with the increased miss parameter and the decreased S_1 concentration in the mutant.

Fluorescence decay

The fluorescence decay after a saturating flash is indicative of the initial rate of Q_A^- reoxidation by the secondary acceptor (fast phase) and of the dark equilibration between $Q_A^-Q_B$ and $Q_AQ_B^-$ (slower phases).

The fluorescence decay can be fitted by a sum of three exponentials.

The half-time of the slow phase was arbitrarily fixed at 1 s. In M_{30} the amplitude of the fast phase was

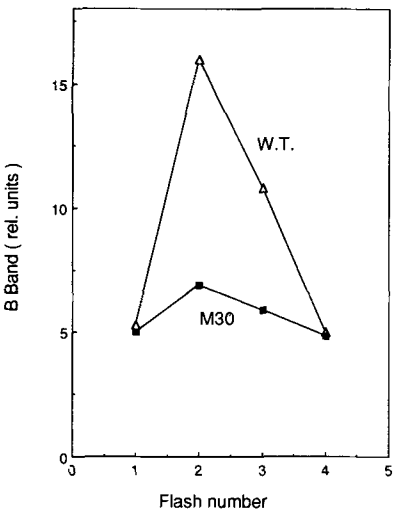

Fig. 7. The oscillation pattern of flash-induced thermoluminescence after a series of flashes in wild-type (△ ——— △) and M_{30} (■ ——— ■) cells.

TABLE III

Fluorescence decay analysis for the wild-type and the M_{30} mutant

	Fast phase amplitude$_1$ (%)	τ_1 (μs)	Medium phase amplitude$_2$ (%)	τ_2 (ms)	Slow phase amplitude$_3$ (%)	τ_3 (s)
Wild-type	73	150	15	1.4	12	1 [a]
M_{30}	64	180	22	1.5	14	1 [a]

[a] The half time of the slow phase is arbitrarily fixed at 1 s.

slightly decreased, and its half-time slightly increased (Table III). The two slower phase amplitudes were increased. Q_A^- reoxidation was slightly slower and the steady state equilibrium was slightly shifted towards Q_A^-.

Discussion

In this report we analyze a metribuzin resistant mutant of *Synechocystis* 6714, M_{30}, which presented a modified distribution of S-states after dark adaptation in addition to changes in the electron transport between Q_A and Q_B.

After dark adaptation, in wild-type cells 30–40% of the centers are in S_0. On the contrary, in M_{30} cells 50–60% of the centers are in S_0 These values are computed from the oxygen sequences where only the S_3 state concentration is measured. The true mechanism of the charge accumulation is not completely resolved and the S_0 and S_1 chemical identification is still an open question.

Three different hypothesis can explain the apparent increase of S_0 concentration in the dark: (1) Reduction of Y_D^+ in the dark and subsequent fast reoxidation by S_2 and S_3 ($t_{1/2}$: 2 s) during the first flashes; (2) oxidation of an accessory electron donor by the first flash; (3) slow dark reduction of S_1 by an unknown reductant present in the cell.

We have shown that the amplitude of the EPR signal II slow was the same in the mutant and in the wild type and that the oscillatory pattern did not depend on the flash frequency. These results demonstrated that a modified interaction between the tyrosine Y_D and the S-states was not the cause of the apparent increase of S_0 concentration.

The oxidation of another component of the PS II (i.e., cytochrome *b*-559) seems improbable, since all the abnormalities in the oxygen oscillatory pattern observed in the M_{30} mutant cells were suppressed in the thylakoids.

Therefore, we favor the hypothesis of a true destabilization of S_1, in the M_{30} mutant. This destabilization may be due to a better accessibility of the oxygen evolving site to reductant molecules. Benzoquinone, a strong oxidant, restored the normal S-state distribution in the mutant. The concentration of the reductant may depend on the oxido-reduction state of the plastoquinone pool, which is known to be oxidized after benzoquinone treatment [36,37]. Almost all the work published on chloroplast or on PS II particles showed that S_1 is very stable in the dark. Only Plijter et al. [38] and Lockett et al. [39] suggested that in PS II particles a high pH destabilizes S_1 which is completely converted to S_0. The situation seems to be different in whole cells where the $S_0 - S_1$ distribution is about 35–40% S_0, 60–65% S_1. This is true not only for cyanobacteria but also for *Chlorella* and *Chlamydomonas reinhardtii* [9]. We suggest that the mechanism leading to an apparent concentration of S_0 larger than the 25% predicted from Kok's model, exists already in the wild-type cells of *Synechocystis*. In the metribuzin resistant mutant, the apparent equilibrium between S_0 and S_1 is shifted in favor of S_0.

In addition to the shift of the apparent equilibrium between S_0 and S_1 towards S_0, the M_{30} mutant has other characteristics also found in the herbicide resistant mutants that were previously characterized in our laboratory. [21]. The electron transfer between Q_A and Q_B is modified by the mutation. Q_A reoxidation is somewhat slower and the apparent steady state equilibrium between $Q_A^-Q_B$ and $Q_AQ_B^-$ is shifted towards $Q_A^-Q_B$. As expected, S_2 deactivation is faster and the B band of thermoluminescence is shifted to lower temperatures.

The shift of the B band was the same in the whole cells and in the thylakoids. However, in the thylakoids, the oxygen oscillatory pattern was normal and the S_2 deactivation was slowed down. These results suggest that in vitro S_2 destabilization is only due to modifications in the acceptor site. In M_{30} cells, the destabilization of the S states can be produced by alterations on the donor and on the acceptor side of the reaction centers. Transformation of the wild type *Synechocystis* 6803 with the mutated genome of M_{30} showed that the mutation(s) generating the metribuzin resistance is also responsible for the modification of the oxygen evolving site.

M_{30} is the first herbicide-resistant mutant described in the literature which presents alterations in the acceptor and donor side of the PS II. All other mutants have a mutated Q_B pocket in D_1, which only modifies the herbicide affinity for the site and the electron

transport between Q_A and Q_B. The new phenotype may be caused by mutation in a different region of the D_1 protein. The search for the mutation is now in progress. Preliminary results suggest that the Q_B pocket is not mutated in the M_{30} mutant (C. Astier, personal communication).

Another metribuzin resistant mutant, M_{35}, which is more resistant to metribuzin and also resistant to atrazine gives the same abnormal pattern for the oxygen sequence. It has not yet been as fully characterized as the M_{30} mutant.

Acknowledgements

We are indebted to Dr. Alain Boussac for discussion and collaboration in the EPR measurement of signal II_{slow} presented in Fig. 2.

References

1 Velthuys, B. (1981) FEBS Lett. 126, 277–281.
2 Wollman, F.A. (1978) Biochim. Biophys. Acta 503, 263–273.
3 Kok, B., Forbush, B. and McGloin, M.P. (1970) Photochem. Photobiol. 11, 457–475.
4 Forbush, B., Kok, 5. and McGloin, M.P. (1971) Photochem. Photobiol. 14, 307–321.
5 Velthuys, B. and Visser, J.W.M. (1975) FEBS Lett. 55, 109–112.
6 Vermaas, W.F.J., Renger, G. and Dohnt, G. (1984) Biochim. Biophys. Acta 764, 194–202.
7 Styring, S. and Rutherford, A.W. (1987) Biochemistry 26, 2401–2405.
8 Vass, I., Deak, Z. and Hideg, E. (1990) Biochim. Biophys. Acta 1017, 63–69.
9 Lavorel, J. (1978) J. Theor. Biol. 57, 171–185.
10 Tischer, W. and Strotmann, H. (1977) Biochim. Biophys. Aacta 460, 113–125.
11 Trebst, A. (1986) Z. Naturforsch. 41c, 240–245.
12 Mets, L. and Thiel, A. (1989) in Target sites of herbicide action (Böger, P. and Thiel, A. , eds.), pp. 2–24, CRC Press, Boca Raton.
13 Ort, D.R., Ahrens, W.H., Martin, B. and Stoller, E.W. (1983) Plant Physiol 72, 925–930.
14 Vermaas, W.F.J. and Arntzen, C.J. (1983) Biochim. Biophys. Acta 725, 483–491.
15 Astier, C., Meyer, I., Vernotte, C. and Etienne, A.L. (1986) FEBS Lett. 207, 234–238.
16 Robinson, H., Golden, S., Brusslan, J. and Haselkorn, R. (1987) in Progress in Photosynthesis Research (Biggins, J., ed.), Vol. 4, pp. 825–828, Martinus Nijhoff, Dordrecht.
17 Erickson, J.M., Pfister, K., Rahire, M., Togasaki, R.K., Mets, L. and Rochaix, J.D. (1989) Plant Cell 1, 361–371.
18 Ajlani, G., Kirilovsky, D., Picaud, M. and Astier, C. (1989) Plant Mol. Biol. 13, 469–479.
19 Kirilovsky, D., Ajlani, G., Picaud, M. and Etienne, A.L. (1989) Plant Mol. Biol. 13, 355–363.
20 Ajlani, G., Meyer, I., Vernotte, C. and Astier, C. (1989) FEBS Lett. 246, 207–210.
21 Etienne, A.L., Ducruet, J.-M., Ajlani, G. and Vernotte, C. (1990) Biochim. Biophys. Acta 1015, 435–440.
22 Bettini, P., McNally, S., Sevignac, M., Darmency, H., Gasquez, J. and Dron, M. (1987) Plant Physiol. 84, 1442–1446.
23 Erickson, J., Rahire, M., Bennoun, P., Delepelaire, P. Diner, B. and Rochaix, J.D. (1984) Proc. Natl. Acad. Sci. USA 81, 3617–3621.
24 Herdman, M., Deloney, S.F. and Carr, N.G. (1973) J. Gen. Microbiol. 79, 233–237.
25 Burnap, R., Koike, H., Sotiropoulou, G., Sherman, L.A. and Inoue, Y. (1989) Photosynth. Res. 22, 123–130.
26 Bouşsac, A. and Etienne, A.L. (1982) Biochim. Biophys. Acta 682, 281–288.
27 Joliot, P. and Joliot, A. (1968) Biochim. Biophys. Acta 153, 625–634.
28 Vass, I., Horvath, G., Herczeg, T. and Demeter, S. (1981) Biochim. Biophys. Acta 634, 140–152.
29 Devault, D., Govindjee and Arnold, W. (1983) Proc. Natl. Acad. Sci USA 80, 983–987.
30 Boussac, A. and Rutherford, A.W. (1988) Biochemistry 27, 3476–3483.
31 Rutherford, A.W., Crofts, A.R. and Inoue, Y. (1982) Biochim. Biophys. Acta 682, 457–465.
32 Demeter, S. and Vass, I. (1984) Biochim. Biophys. Acta 764, 24–32.
33 Inoue, Y. (1983) in The oxygen evolving system of photosynthesis (Inoue, Y., Crofts, A.R., Govindjee, Murata, N., Renger, G. and Satoh, K., eds.), pp. 439–450, Academic Press, Tokyo.
34 Rutherford, A.W., Renger, G., Koike, H. and Inoue, Y. (1984) Biochim. Biophys. Acta 767, 548–556.
35 Govindjee, Koike, H. And Inoue, Y. (1985) Photochem. Photobiol. 42, 579–585.
36 Lavergne, J. (1984) FEBS Lett. 173, 9–14.
37 Joliot, P. and Joliot, A. (1985) Biochim. Biophys. Acta 806, 398–409.
38 Plijter, J.J., De Groot, A., Van Dijk, M.A. and Van Gorkom, H.J. (1986) FEBS Lett. 195, 313–318.
39 Lockett, C.J., Demetriou, C., Bavden, S.J. and Nugent, J.H.A. (1990) Biochim. Biophys. Acta 1016, 213–218.